GEOLOGY | THE GEOLOGICAL SOCIETY OF AMERICA®

https://doi.org/10.1130/G50165.1

Manuscript received 11 October 2021
Revised manuscript received 26 February 2022
Manuscript accepted 2 March 2022

Published online 26 April 2022

Possible bipolar global expression of the P3 and P4 glacial events of eastern Australia in the Northern Hemisphere: Marine diamictites and glendonites from the middle to upper Permian in southern Verkhoyanie, Siberia

V.I. Davydov[1,2,3]*, I.V. Budnikov[4], R.V. Kutygin[5], N.G. Nurgalieva[3], A.S. Biakov[6], E.V. Karasev[3,7], A.N. Kilyasov[5] and V.I. Makoshin[5]

[1]Institute of Petroleum Geology and Geophysics, Siberian Branch, Russian Academy of Sciences, Prospect Ac. Koptjuga 3, Novosibirsk 630090, Russia
[2]Department of Geosciences, Boise State University, 1910 University Drive, Boise, Idaho 83725, USA
[3]Department of Stratigraphy and Paleontology, Kazan Federal University, 18 Kremlyovskaya Street, Kazan, Republic of Tatarstan 420008, Russia
[4]Siberian Research Institute of Geology, Geophysics and Mineral Resources, 67 Krasnyj pr., Novosibirsk 630091, Russia
[5]Diamond and Precious Metal Geology Institute, Siberian Branch, Russian Academy of Sciences, 39 Lenina Prospect, Yakutsk 677891, Russia
[6]North-East Interdisciplinary Scientific Research Institute, Russian Academy of Sciences, Magadan 685000, Russia
[7]Paleontological Institute, Russian Academy of Sciences, Leninskyi Prospect, Moscow 117997, Russia

ABSTRACT

Three intervals of glaciomarine diamictites with extensive glendonites in middle to upper Permian sediments were found in the Kobyume River, southern Verkhoyanie, Russia. The successions are biostratigraphically constrained as middle to upper Permian. The middle Permian diamictite horizons extend over a large area with a lateral distance of >1000 km. The upper Permian diamictites developed only locally. The diamictites are interpreted as glaciomarine sediments containing ice-rafted debris. Two glacial episodes in Siberia temporally correspond to the P3 (middle Permian) and P4 (late Permian) glacial events of eastern Australia, strongly suggesting a global bipolar climate and well-developed climatic belts during the middle to late Permian.

INTRODUCTION

The Late Paleozoic Ice Age (LPIA) was one of the most pronounced and intensive of the four global Phanerozoic glaciations. The most extensive record of the LPIA came from the Southern Hemisphere, i.e., Gondwanan glaciation, where glacial deposits of Carboniferous and early Permian age are widespread. The middle and late Permian glaciation episodes (P3 and P4 alpine glaciations) have been described as only local and/or regional to eastern Australia (Fielding et al., 2008a, 2008b; Isbell et al., 2012).

Climatic models for the Carboniferous and Permian support the prospect of bipolar glaciation (Hyde et al., 2006; Montañez and Poulsen, 2013), but both the nature and extent of Northern Hemisphere ice remain elusive. We report extensive middle to late Permian marine facies with glendonites and possible glaciomarine diamictites in the Kobyume River, southern Verkhoyanie, Russia (Figs. 1 and 2; Figs. S1–S9 in the Supplemental Material[1]).

GEOLOGICAL SETTING

The Verkhoyanie fold-thrust system consists of an S-shaped belt between the Lena and Indigirka Rivers (Fig. 1; Fig. S1). The system developed on the passive margin of the Siberian craton and comprises late Precambrian to Jurassic terrestrial and marine rocks deposited on crystalline Precambrian basement. During the middle to late Permian, the southern Verkhoyanie was at high latitudes (~65–70°N) (Fig. 1). The glaciomarine sediments in Siberia contain ice-rafted debris (IRD) similar to that reported in the modern-day Arctic seas and Arctic Ocean (Lisitzin, 2002). In the latter, water exists as a solid phase most of the year, both in submarine drainage systems and on the sea surface. The environments on the Arctic Ocean shelf are characterized by perennial permafrost. Biogenic processes in the modern-day IRD sediments have had minimum effect on sediments because of the long polar night and because ice blocks photosynthesis (Lisitzin, 2002). No evidence of terrestrial glaciation during the Permian has ever been reported in Siberia. IRD can be incorporated into sediments without the influence of glaciers (Isbell et al., 2021).

PERMIAN STRATIGRAPHY AND ENVIRONMENTS OF THE KOBYUME RIVER

The thick Permian siliciclastic succession at the Kobyume River (~2900 m) (Fig. 2; Figs. S2–S6) includes (upward) the Kobyume, Tiryakh, Lugovaya, Privolnyi, and Nekuchan Formations (Abramov, 1974) (see details of the litho- and biostratigraphy in the Supplemental

*E-mails: vdavydov@boisestate.edu; DavydovVI@ipgg.sibras.ru

[1]Supplemental Material. Lithostratigraphy, biostratigraphy and age control; Table S1 (distribution and taxonomy of the fossils in the Kobume section, Verkhoyanie, Russia); and supplemental Figures S1– S23. Please visit https://doi.org/10.1130/GEOL.S.19579360 to access the supplemental material, and contact editing@geosociety.org with any questions.

CITATION: Davydov, V.I., et al., 2022, Possible bipolar global expression of the P3 and P4 glacial events of eastern Australia in the Northern Hemisphere: Marine diamictites and glendonites from the middle to upper Permian in southern Verkhoyanie, Siberia: Geology, v. XX, p. , https://doi.org/10.1130/G50165.1

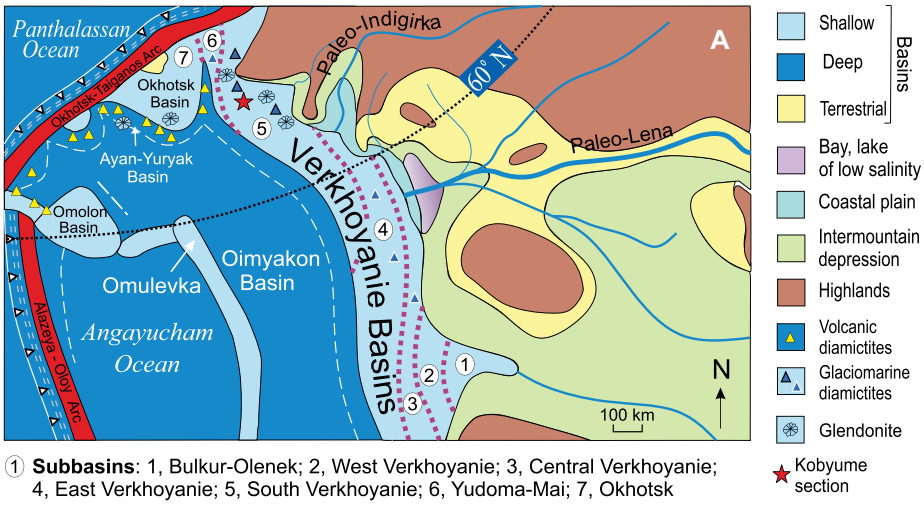

① **Subbasins**: 1, Bulkur-Olenek; 2, West Verkhoyanie; 3, Central Verkhoyanie; 4, East Verkhoyanie; 5, South Verkhoyanie; 6, Yudoma-Mai; 7, Okhotsk

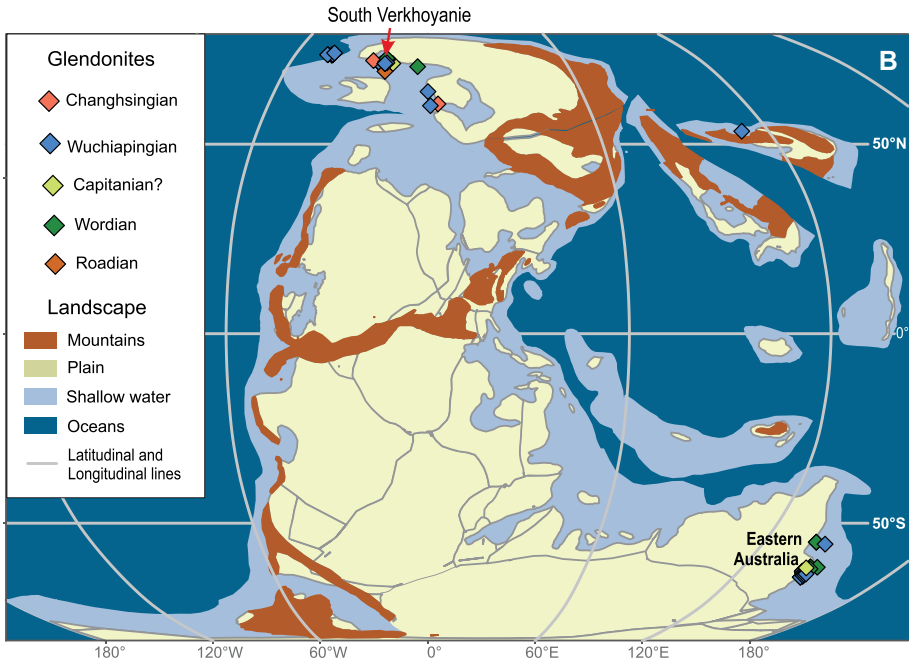

Figure 1. (A) Paleogeography of the Verkhoyanie Basin (present-day northeast Russia) and surrounding areas during the middle to late Permian. Note that the north direction in the Permian corresponds to the south direction in present day. (B) Distribution of glendonites within high latitudes in Pangean seas (Matthews et al., 2016). Data are from the Rogov et al. (2021) database, but were corrected with regard to a recent chronostratigraphy (Davydov et al., 2018; Budnikov et al., 2020; Kutygin et al., 2020; Biakov et al., 2021).

Material). The lower Nekuchan Formation, which encompasses the Permian-Triassic boundary, comprises well-bedded siltstone with numerous cherty carbonate ellipsoidal concretions and rare beds of fine- to medium-grained sandstone in 0.5–3-m-thick beds (Kutygin et al., 2019) (Fig. 2; Fig. S6). The entire Permian succession at the Kobyume River reveals deposition in prodelta to delta-plain sedimentary settings with mouth sand bars (Figs. S2–S7) and with no signs of sedimentary gaps in the sequence. The succession progressively shallows upward and becomes very shallow in the middle to upper Privolnyi Formation, where wood and floral debris is found (see Figs. S2–S6 for all samples collected in the succession). All samples were collected along the bottom of the river cut in a distance of ~5 km. Sedimentation rates in the Permian of the Kobyume section are generally uniform throughout (Fig. 2). The entire Permian succession is driven by eustacy (Fig. 2; Fig. S7). Glaciogenic cyclopels and cyclopsams (graded sand-mud couplets) (Mackiewicz et al., 1984) are rare and found only in the lower Tiryakh Formation (Fig. S9). A progressive increase in cycle thickness (decimeter to meter) in the Kobyume section is associated with sea-level fluctuations (allocycles) that shallow (coarsening sediments) upward. No Bouma cycles with fining-upward beds or chaotic and/or folded strata were recognized in the section. Asymmetric (0.3–04 m) and linguoid (0.15–0.2 m) ripple marks at the top of the allocycles are rare in the Kobyume Formation and more common the Tiryakh Formation (Fig. 2; Fig. S10) and indicate environments close to wave base (20–80 m) or shallower. Ripple marks, subaqueous cracks, and hummocky and cross-bedding structures are frequent in the Lugovaya and Privolnyi Formations (Fig. 2; Figs. S10 and S11).

GLENDONITES IN THE KOBYUME SECTION

Glendonites (calcite pseudomorphs after the metastable mineral ikaite, $CaCO_3 \cdot 6H_2O$, crystallized at a temperature <4–6 °C with normal marine pH) are unevenly distributed in the Kobyume section (Figs. 2 and 3G–3J; Fig. S8). Their morphology varies from horizon to horizon, but star-like rosette shapes are most common and stellate crystals are rare (Figs. 3G–3J; Fig. S8). The glendonites in the Kobyume section generally occur below and above the diamictites (Fig. 2). The stable isotope composition ($\delta^{13}C$ and $\delta^{18}O$) of the glendonites shows a negative covariance, with $\delta^{13}C$ values ranging from +2.94‰ to −14.11‰ and $\delta^{18}O$ values from −13.96‰ to −26.37‰ (Fig. 4). Isotopically, the Permian glendonites from the Kobyume section slightly overlap with those from eastern Australia (Frank et al., 2008, 2015) and generally have a lighter $\delta^{18}O$ value (Fig. 4) that suggests a slight diagenetic overprint (Popov et al., 2019).

MIDDLE TO LATE PERMIAN DIAMICTITES IN THE KOBYUME SECTION

Two types of diamictites are recognized in the Kobyume section: (1) ice-proximal, massive to coarsely bedded diamictites in the Tiryakh Formation (Figs. 3A–3D; Figs. S12–S16); and (2) ice-distal, laminated, clast-poor diamictites in the Privolnyi Formation (Figs. 3E and 3F; Fig. S17). The Tiryakh diamictites form massive, stratified beds from 0.5 m up to 20–30 m thick (Fig. S12). Glaciomarine diamictites are composed of two components: the dominant fines (clay, mud, and fine sand) settling from meltwater plumes, and coarse material released from IRD (Powell, 1990). Clast to matrix (silt) ratio ranges from 0.15 to 0.40. The clasts are composed of igneous, carbonate, sandstone, and rare cherty boulders as much as 1.0 m in length. Striated clasts are very rare (Fig. 3D), and lack of striated clasts is characteristic for IRD (Lisitzin, 2002). The greenish-gray matrix is fine siltstone with a minor volcaniclastic component. Rounded clasts are predominant in the glaciomarine sediments at the Kobyume section, but faceted polygonal clasts are also common (Fig. 3C; Figs. S13A–S13B, S14B, and S15C). IRD commonly penetrates soft sediments at an angle or perpendicular to the

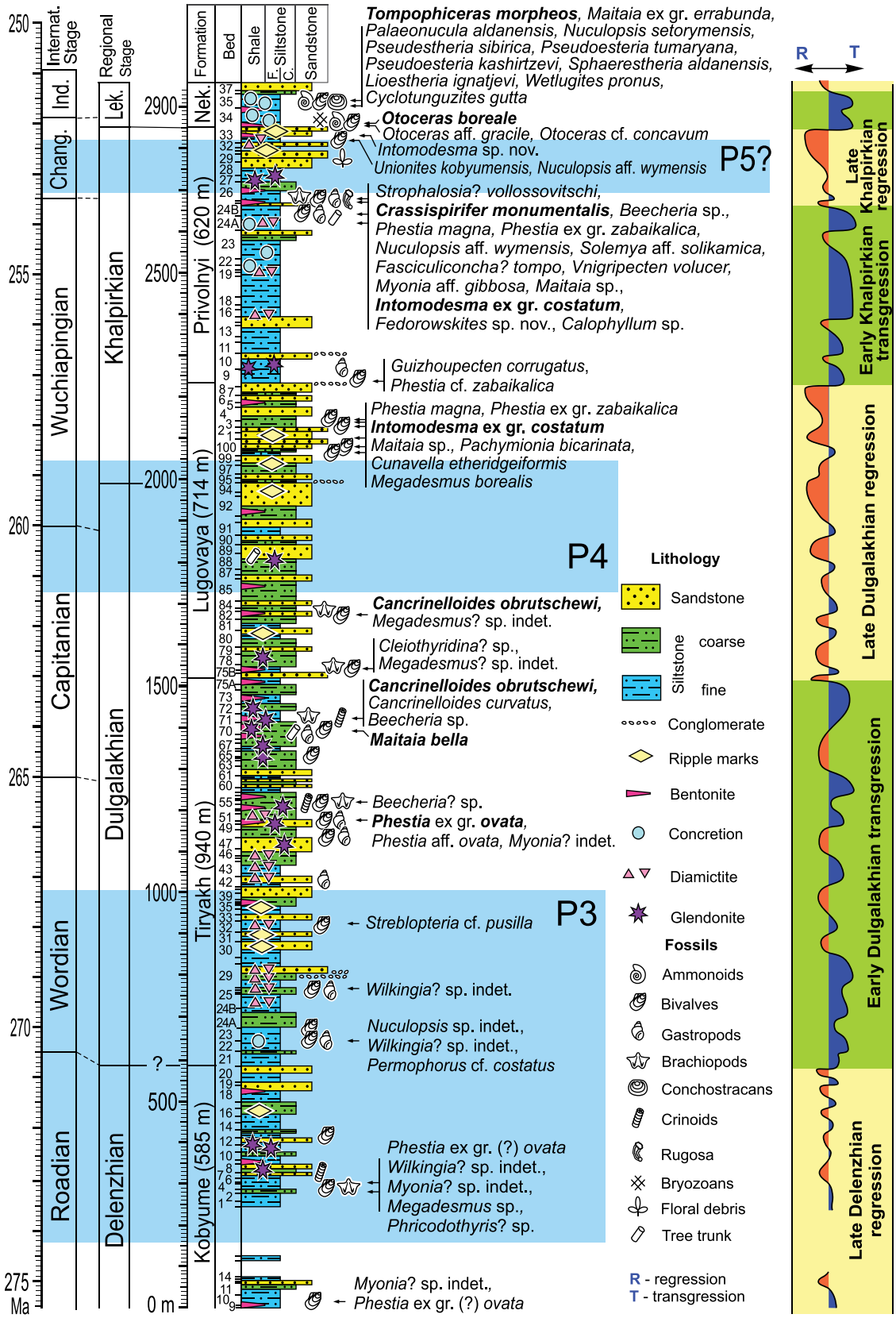

Figure 2. Stratigraphic log of middle to upper Permian and Lower Triassic deposits along the Tiryakh-Yuryakh and Kobyume Rivers, Siberia (Fig. S1 [see footnote 1], locations 19R1, 2u/16–19R2, and 3u16–19R3). Abbreviations: Internat.—International; Ind.—Induan; Chang.—Changhsingian; Lek.—Lekeerian; Nek.—Nekuchan; F.—Fine; C.—Coarse. Most diagnostic fossils are in bold font. Shaded blue areas indicate global glacial episodes in eastern Australia and cooling events elsewhere.

bedding (Figs. 3A and 3C; Figs. S13A–S13B, S15B–S15C, and S16B).

Black, clast-poor diamictites in the Privolnyi Formation occur as repeated stratigraphic tabular horizons intercalated with siltstone and fine sandstone (Figs. 3E and 3F; Fig. S17 and S17B–S17D). The deposits consist of fine-stratified mudstones with isolated, well-rounded, medium and small quartzite and silty carbonate clasts (dropstones) as much as 7 cm in diameter that interrupt the lamination (Figs. 3E and 3F). Clast proportion relative to matrix varies from 0.5% to 2%–3% and passes gradationally into the normal siltstone-mudstone. These clast-poor diamictites are expressed at the Kobyume section as two

horizons: the lower is 30–35 m thick, and the upper is 3–5 m thick (Fig. 2).

DISCUSSION

The Permian paleogeographic configuration of the Siberian platform and Verkhoyanie Basin (passive margin of the platform) suggest that the current southern Verkhoyanie and Okhotsk Basins were at more northerly latitudes than the present day central and northern Verkhoyanie Basin (Fig. 1A; Fig. S1A). The abundant diamictites and glendonites in the middle to upper Permian of the Kobyume section indicate two to three climatic glacial episodes. The occurrence of relatively diverse fauna throughout the succession (Fig. 2; Figs. S18–S23) indicates normal marine salinity and pH (8.0–8.2). During the Permian, the southern Verkhoyanie Basin was in the northern end of the foredeep at ~65–70°N latitude. The temperature of the modern-day shallow water at these latitudes in the Arctic varies from 0 to −1.7°C, and the shallow marine water has lower pH (7.4–8.0) (Lisitzin, 2002).

Prominent glaciation-deglaciation cycles are recognized in the distribution of the glendonites and diamictites in the Kobyume section. The glendonites first occur in the middle Kobyume Formation, indicating a potential onset of a glacial episode (Fig. 2). Glendonites disappear in the upper Kobyume Formation (lower Guadalupian?) below the massive diamictites of the Tiryakh Formation, which indicate the initiation an interval of glacial retreat (Fig. 2) (Powell and Cooper, 2002; Birgenheier et al., 2009). In the upper Tiryakh Formation, diamictites are absent but glendonites are common again. The Lugovaya Formation is generally free from both glendonites and diamictites (Fig. 2). The climate interpretation for the time of Lugovaya Formation deposition is controversial. On one hand, the abundance of the fossils suggests a warmer climate, but the major regression and sea-level fall in the region suggests a glaciation episode. This problem could be resolved with the better constraints from U-Pb dates to be obtained soon by us (Fig. S18). Clast-poor diamictites appear again in the lower Privolnyi Formation (2400–2650 m; Fig. 2; Fig. S6). Abundant fossils, including *Fedorowskites* and *Calophyllum rugosa* corals, occur immediately above these diamictites, indicating a brief climate warming pulse. The abundant glendonites occur again in thin (3–5 m) horizons, 10–12 m above the fauna-rich bed, suggesting another potential glacial episode. Another 3–5-m-thick horizon of clast-poor diamictites occurs near the top of the Privolnyi Formation (Fig. 2; Fig. S6).

The middle Permian diamictites from Kobyume River extend laterally over a large area northward for 600–700 km (Dyanyshka and Echyi Rivers), where the diamictites become thinner (<100 m) and gradually disappear toward the modern-day northern Verkhoyanie Basin (Fig. 1A; Fig. S1A) (Andrianov, 1966; Abramov, 1974). The diamictite-bearing Kobyume River succession can be traced to the modern-day south (north in the Permian) in the upper reaches of the Yudoma River (Yudoma-Mai zone) (Fig. 1A; Fig. S1A) (Shekman and Gagen-Torn, 1979; Kanaev et al., 1988). The Yudoma River diamictites (as much as 600 m thick) accumulated in a shallow-water setting, commonly with well-preserved plant

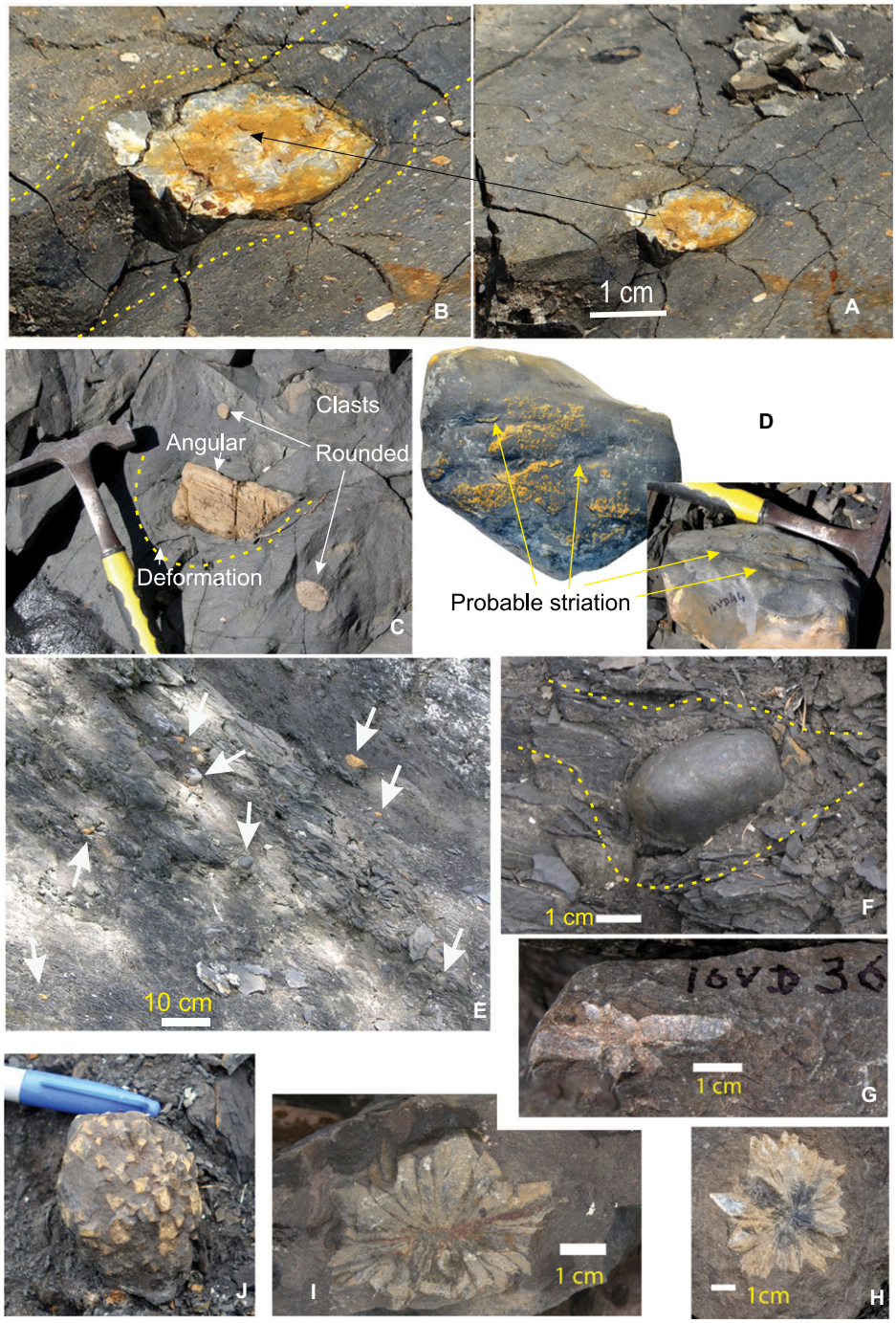

Figure 3. Diamictite and glendonites from the middle and upper Permian at the Kobyume River (Siberia) section (the studied section was at the river cut, where it is best exposed). (A–D) Middle Permian diamictites. (A) Quartz pebble within laminated matrix (sampled at 715 m above the base of the section). (B) Closer view of the pebble in A with clear deformation of laminated matrix. (C) Angular and rounded dropstone with deformation surrounding boulder and pebbles (at 805 m). (D) Large boulder (collected at 1190 m) with probable striation; no fracture or cracks are observed in this boulder. (E) Wuchiapingian clast-poor diamictites; white arrows point to rounded pebbles within mudstone (collected at 2080 m). (F) Wuchiapingian cherty dropstone within deformed laminated matrix (collected at 2083 m). (G–I) Rosette and stellate middle Permian glendonites. (G: collected at 390 m; H: collected at 1453 m; I: collected at 1448 m.) (J) Wuchiapingian glendonite (collected at 2785 m).

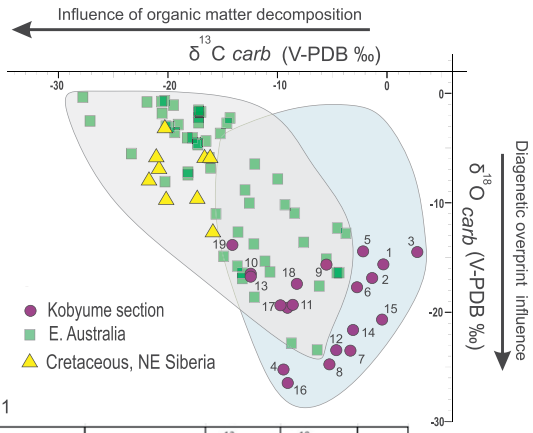

Table 1

No;	Sample No;	Height above section base (m)	$\delta^{13}C_{carb}$ V-PDB ‰	$\delta^{18}O_{carb}$ V-PDB, ‰	TOC%
1	16 VD34	337	-0.33	-15.69	1.07
2	19R2-8-os	338	-1.45	-16.93	1.71
3	16 VD36	391	2.94	-14.50	1.62
4	16 VD37	405	-9.53	-25.25	0.99
5	16 VD45	1119	-2.22	-14.50	0.72
6	19R2-47-12	1123	-2.76	-17.61	0.48
7	19R2-70-13.7p	1401.7	-4.66	-23.70	0.64
8	19VD-27	1403	-5.27	-24.63	0.42
9	19R2-70-20p	1408	-5.37	-16.31	0.50
10	16VD50a	1426.0	-12.53	-16.50	0.83
11	16VD48	1447	-8.64	-19.22	0.71
12	19R2-72-14.5	1452.5	-4.79	-23.49	0.50
13	16VD53	1455	-12.53	-16.50	0.52
14	19R2-78-17.5	1577.5	-3.05	-21.61	0.53
15	19R2-78-17.5p	1574.5	-3.03	-20.78	0.64
16	19VD35	1812	-9.01	-26.37	0.70
17	16VD53	2694	-9.64	-19.60	0.50
18	16VD53A	2698	-8.20	-17.30	0.75
19	16 VD55	2716	-14.11	-13.96	1.11

Figure 4. Comparison of $\delta^{13}C$ and $\delta^{18}O$ stable isotopes of glendonites from the Kobyume River (Siberia) section, at the river cut exposure, with those from the Permian of eastern Australia (Frank et al., 2008, 2015) and with isotopes of Cretaceous glendonites from Siberia (Rogov et al., 2017). Isotopically, glendonites from the Kobyume River are similar to Permian glendonites in eastern Australia, but do not overlap Cretaceous samples; the latter are less altered than the former. Photo shows glendonites from the upper Lugovaya Formation, sample 19VD35 (#16 in the table), collected at 1812 m. carb—carbonate; V-PDB—Vienna Peedee belemnite; TOC—total organic carbon.

fossils (Shekman and Gagen-Torn, 1979). Glendonites have not yet been recognized in that area.

The thickness and lateral distribution (~1000 km) of the middle Permian diamictites suggest that the associated climatic glacial event in Siberia was significant. The current biostratigraphy in the area suggests a middle and possibly late Guadalupian age for this event in Verkhoyanie. This climatic episode temporally corresponds with the middle Guadalupian P3 glacial event in eastern Australia (Fig. 2) (Fielding et al., 2008b; Frank et al., 2015; Metcalfe et al., 2015; Laurie et al., 2016; Davydov et al., 2018; Phillips et al., 2018).

The second, late Permian, glacial event is documented in the current study area and to the southwest for a distance of ~100–200 km toward the East Khandyga, Dyby, and Yudoma Rivers (Kanaev et al., 1988; Afanasiev and Gorlova, 2013). This event is expressed in the Kobyume section as clast-poor diamictites and glendonites (Figs. 2, 3E, 3F, and 3J) and biostratigraphically constrained as early late Permian (Wuchiapingian), therefore correlating with the P4 glacial event of eastern Australia (Metcalfe et al., 2015; Davydov et al., 2018).

The onset of the third, and very small, glaciomarine episode observed near the top of the Permian (Changhsingian) is expressed by the two glendonite horizons at 2700 m (Fig. 2; Fig. S7). This late Changhsingian glacial event has not been recognized in eastern Australia. However, a significant climatic cooling event near the end of the Changhsingian was documented from geochemical and biotic proxies at the Permian-Triassic Global Boundary Stratotype Section and Point (GSSP) at the Meishan section in southern China (Chen et al., 2016), in western China (Liu et al., 2022), in the Moscow Basin of Russia (Davydov et al., 2020), and in South Africa (Rey et al., 2016).

Both the P3 and P4 glacial events in eastern Australia are the alpine type, locally developed within an orogenic belt (Fielding et al., 2008a), whereas in Siberia, the glacial events are expressed as glaciomarine IRD sediments originating from perennial oceanic and coastal sea ice, similar to the setting in the present-day Arctic Ocean and northern coast of Siberia and Russian Far East (Lisitzin, 2002). These rocks have been designated as a new marine ice-rafting type that does not require the presence of a continental glacial mass nearby (Lisitzin, 2002; Tremblay et al., 2015; Isbell et al., 2021).

The difference in the scale and expression of the Guadalupian cooling episode in the Southern and Northern Hemispheres can be explained by their paleogeographic position. Eastern Australia basins during the middle to late Permian were located at ~55–60°S, whereas the southern Verkhoyanie Basin was at ~65–70°N (Fig. 1B). This means that the equilibrium-line altitude in Siberia was close to or at the shoreline, whereas in eastern Australia, it was within moderately high mountains. In eastern Australia, the P3 glacial event is stronger and of greater scale than the P4 event, and this coincides with observations in southern Verkhoyanie. The onset of both glacial episodes in the Kobyume section corresponds with a sea-level lowstand, and diamictites occur during a highstand (Fig. 2), which also mirrors the sea-level fluctuations during the P3 and P4 glaciations in eastern Australia (Fielding et al., 2008a, 2008b; Frank et al., 2015).

The assumption that "The paleo-arctic region was totally oceanic during the Paleozoic" (González and Díaz Saravia, 2010, p. 108) is therefore not supported, at least for middle to late Permian time. Rather, the occurrence of middle to late Permian glaciomarine sediments in Siberia is consistent with the proposed global Köppen-Geiger climate classification (Kottek et al., 2006) and more recent bipolar climatic models (Hyde et al., 2006; Montañez and Poulsen, 2013). The Köppen-Geiger model of the present-day climatic belts and biomes, therefore, can be extended into deep time toward at least the middle to late Permian. In the Southern Hemisphere, the Carboniferous and early Permian glacial events were much more strongly developed and widely distributed than in the middle to late Permian (Rosa and Isbell, 2021). The analogues of these events potentially could be found in Siberia. Further study of potential upper Paleozoic glacial events and paleogeography in these very remote areas of Siberia is essential.

ACKNOWLEDGMENTS

Financial support was provided to all authors by the Russian Scientific Foundation (RSF), project 19-17-00178. This study is a part of the Ministry of Science and Higher Education of Russia project FWZZ-2022-0005 (to V. Davydov) performed by the Institute of Petroleum Geology and Geophysics, Novosibirsk. Identification of rugosa corals by O.L. Kossovaya from the All-Russian Geology Scientific Research Institute (VSEGEI, St. Petersburg), is highly appreciated. We thank students and individuals from Kazan Federal University for help with different aspects of project development. We appreciate the help of Walter S. Snyder from Boise State University (Idaho, USA) with English improvement. We thank John. L. Isbell for his comments on the first draft of the manuscript. Three anonymous reviewers made many valuable suggestions that improved the final version of the manuscript, and editor Gerald Dickens provided inspired comments.

REFERENCES CITED

Abramov, B.S., 1974, Stratigraphy of the Upper Paleozoic of Southern Verkhoyanie: Novosibirsk, Nauka, 102 p. (in Russian).

Afanasiev, M.G., and Gorlova, A.L., 2013, State geological map of Russia, Udoma series,

sheet P54-XIX: Explanatory notes: Moscow, All-Russian Scientific Research Institute (VSEGEI), scale 1:200,000, 215 p. (in Russian).

Andrianov, V.N., 1966, Verkhnepaleozoiskie otlozheniya Zapadnogo Verkhoyan'ya (Upper Paleozoic Sediments of the Western Verkhoyanie Region): Moscow, Nauka, 136 p. (in Russian).

Biakov, A.S., Zakharov, Yu.D., Horacek, M., and Goryachev, N.A., 2021, The Position of the Wuchiapingian–Changhsingian boundary in northeast Russia on the basis of radioisotopic and chemostratigraphic data: Doklady Earth Sciences, v. 500, p. 816–819, https://doi.org/10.1134/S1028334X21100056.

Birgenheier, L.P., Fielding, C.R., Rygel, M.C., Frank, T.D., and Roberts, J., 2009, Evidence for dynamic climate change on sub-106-year scales from the late Paleozoic glacial record, Tamworth Belt, New South Wales, Australia: Journal of Sedimentary Research, v. 79, p. 56–82, https://doi.org/10.2110/jsr.2009.013.

Budnikov, I.V., Kutygin, R.V., Shi, G.R., Sivtchikov, V.E., and Krivenko, O.V., 2020, Permian stratigraphy and paleogeography of Central Siberia (Angaraland)–A review: Journal of Asian Earth Sciences, v. 196, 104365, https://doi.org/10.1016/j.jseaes.2020.104365.

Chen, J., et al., 2016, High-resolution SIMS oxygen isotope analysis on conodont apatite from South China and implications for the end-Permian mass extinction: Palaeogeography, Palaeoclimatology, Palaeoecology, v. 448, p. 26–38, https://doi.org/10.1016/j.palaeo.2015.11.025.

Davydov, V.I., Biakov, A.S., Schmitz, M.D., and Silantiev, V.V., 2018, Radioisotopic calibration of the Guadalupian (middle Permian) series: Review and updates: Earth-Science Reviews, v. 176, p. 222–240, https://doi.org/10.1016/j.earscirev.2017.10.011.

Davydov, V.I., Arefiev, M.P., Golubev, V.K., Karasev, E.V., Naumcheva, M.A., Schmitz, M.D., Silantiev, V.V., and Zharinova, V.V., 2020, Radioisotopic and biostratigraphic constraints on the classical Middle–Upper Permian succession and tetrapod fauna of the Moscow syneclise, Russia: Geology, v. 48, p. 742–747, https://doi.org/10.1130/G47172.1.

Fielding, C.R., Frank, T.D., Birgenheier, L.P., Rygel, M.C., Jones, A.T., and Roberts, J., 2008a, Stratigraphic record and facies associations of the late Paleozoic ice age in eastern Australia (New South Wales and Queensland), *in* Fielding, C.R., et al., eds., Resolving the Late Paleozoic Ice Age in Time and Space: Geological Society of America Special Paper 441, p. 41–57, https://doi.org/10.1130/2008.2441(03).

Fielding, C.R., Frank, T.D., and Isbell, J.L., 2008b, The late Paleozoic ice age—A review of current understanding and synthesis of global climate patterns, *in* Fielding, C.R., et al., eds., Resolving the Late Paleozoic Ice Age in Time and Space: Geological Society of America Special Paper 441, p. 343–354, https://doi.org/10.1130/2008.2441(24).

Frank, T.D., Thomas, S.G., and Fielding, C.R., 2008, On using carbon and oxygen isotope data from glendonites as paleoenvironmental proxies: A case study from the Permian System of eastern Australia: Journal of Sedimentary Research, v. 78, p. 713–723, https://doi.org/10.2110/jsr.2008.081.

Frank, T.D., Shultis, A.I., and Fielding, C.R., 2015, Acme and demise of the late Palaeozoic ice age: A view from the southeastern margin of Gondwana: Palaeogeography, Palaeoclimatology, Palaeoecology, v. 418, p. 176–192, https://doi.org/10.1016/j.palaeo.2014.11.016.

González, C.R., and Díaz Saravia, P., 2010, Bimodal character of the Late Paleozoic glaciations in Argentina and bipolarity of climatic changes: Palaeogeography, Palaeoclimatology, Palaeoecology, v. 298, p. 101–111, https://doi.org/10.1016/j.palaeo.2010.06.011.

Hyde, W.T., Grossman, E.L., Crowley, T.J., Pollard, D., and Scotese, C.R., 2006, Siberian glaciation as a constraint on Permian-Carboniferous CO_2 levels: Geology, v. 34, p. 421–424, https://doi.org/10.1130/G22108.1.

Isbell, J.L., Henry, L.C., Gulbranson, E.L., Limarino, C.O., Fraiser, M.L., Koch, Z.J., Ciccioli, P.L., and Dineen, A.A., 2012, Glacial paradoxes during the late Paleozoic ice age: Evaluating the equilibrium line altitude as a control on glaciation: Gondwana Research, v. 22, p. 1–19, https://doi.org/10.1016/j.gr.2011.11.005.

Isbell, J.L., et al., 2021, Evaluation of physical and chemical proxies used to interpret past glaciations with a focus on the late Paleozoic Ice Age: Earth-Science Reviews, v. 221, 103756, https://doi.org/10.1016/j.earscirev.2021.103756.

Kanaev, A.P., Poligona, S.I., Belyankin, V.I., Arkhangelskaya, V.A., and Kanaeva, G.M., 1988, State geological map of the USSR, Pre-Okhotie series, sheets P54-XXI, XXVII, XXXIII: Explanatory notes: Moscow, All-Union Scientific Research Institute (VSEGEI), scale 1:200,000, 151 p. (in Russian).

Kottek, M., Grieser, J., Beck, C., Rudolf, B., and Rubel, F., 2006, World map of the Köppen-Geiger climate classification updated: Meteorologische Zeitschrift (Berlin), v. 15, p. 259–263, https://doi.org/10.1127/0941-2948/2006/0130.

Kutygin, R.V., Budnikov, I.V., Biakov, A.S., Davydov, V.I., Kilyasov, A.N., and Silantiev, V.V., 2019, The discovery of the first Otoceras (Ceratitida) in the Kobyuma zone of the Southern Verkhoyanie region, Northeastern Russia: Scientific Notes of Kazan Federal University, Natural Science Series, v. 161, p. 550–570, https://doi.org/10.26907/2542-064X.2019.4.550-570 (in Russian).

Kutygin, R.V., Biakov, A.S., Makoshin, V.I., Budnikov, I.V., Peregoedov, L.G., and Krivenko, O.V., 2020, Biostratigraphy and important biotic events in the western Verkhoyansk Region around the Sakmarian–Artinskian boundary: Palaeoworld, v. 29, p. 303–324, https://doi.org/10.1016/j.palwor.2018.10.001.

Laurie, J.R., et al., 2016, Calibrating the middle and late Permian palynostratigraphy of Australia to the geologic time-scale via U–Pb zircon CA-IDTIMS dating: Australian Journal of Earth Sciences, v. 63, p. 701–730, https://doi.org/10.1080/08120099.2016.1233456.

Lisitzin, A.P., 2002, Sea-Ice and Iceberg Sedimentation in the Ocean: Berlin, Springer-Verlag, 563 p., https://doi.org/10.1007/978-3-642-55905-1.

Liu, J., Abdala, F., Angielczyk, K.D., and Sidor, C.A., 2022, Tetrapod turnover during the Permo-Triassic transition explained by temperature change: Earth-Science Reviews, v. 224, 103886, https://doi.org/10.1016/j.earscirev.2021.103886.

Mackiewicz, N.E., Powell, R.D., Carlson, P.R., and Molnia, B.F., 1984, Interlaminated ice-proximal glacimarine sediments in Muir Inlet, Alaska: Marine Geology, v. 57, p. 113–147, https://doi.org/10.1016/0025-3227(84)90197-X.

Matthews, K.J., Maloney, K.T., Zahirovic, S., Williams, S.E., Seton, M., and Müller, R.D., 2016, Global plate boundary evolution and kinematics since the late Paleozoic: Global and Planetary Change, v. 146, p. 226–250, https://doi.org/10.1016/j.gloplacha.2016.10.002.

Metcalfe, I., Crowley, J.L., Nicoll, R.S., and Schmitz, M., 2015, High-precision U-Pb CA-TIMS calibration of Middle Permian to Lower Triassic sequences, mass extinction and extreme climate-change in eastern Australian Gondwana: Gondwana Research, v. 28, p. 61–81, https://doi.org/10.1016/j.gr.2014.09.002.

Montañez, I.P., and Poulsen, C.J., 2013, The late Paleozoic ice age: An evolving paradigm: Annual Review of Earth and Planetary Sciences, v. 41, p. 629–656, https://doi.org/10.1146/annurev.earth.031208.100118.

Phillips, L.J., Crowley, J.L., Mantle, D.J., Esterle, J.S., Nicoll, R.S., McKellar, J.L., and Wheeler, A., 2018, U-Pb geochronology and palynology from Lopingian (upper Permian) coal measure strata of the Galilee Basin, Queensland, Australia: Australian Journal of Earth Sciences, v. 65, p. 153–173, https://doi.org/10.1080/08120099.2018.1418431.

Popov, L.E., et al., 2019, Glendonite occurrences in the Tremadocian of Baltica: First Early Palaeozoic evidence of massive ikaite precipitation at temperate latitudes: Scientific Reports, v. 9, 7205, https://doi.org/10.1038/s41598-019-43707-4.

Powell, R.D., 1990, Glacimarine processes at grounding-line fans and their growth to ice-contact deltas, *in* Dowdeswell, J.A., and Scourse, J.D., eds., Glacimarine Environments: Processes and Sediments: Geological Society, London, Special Publication 53, p. 53–73, https://doi.org/10.1144/GSL.SP.1990.053.01.03.

Powell, R.D., and Cooper, J.M., 2002, A glacial sequence stratigraphic model for temperate, glaciated continental shelves, *in* Dowdeswell, J.A., and Ó Cofaigh, C., eds., Glacier-Influenced Sedimentation on High-Latitude Continental Margins: Geological Society, London, Special Publications 203, p. 215–244, https://doi.org/10.1144/GSL.SP.2002.203.01.12.

Rey, K., et al., 2016, Global climate perturbations during the Permo-Triassic mass extinctions recorded by continental tetrapods from South Africa: Gondwana Research, v. 37, p. 384–396, https://doi.org/10.1016/j.gr.2015.09.008.

Rogov, M.A., Ershova, V.B., Shchepetova, E.V., Zakharov, V.A., Pokrovsky, B.G., and Khudoley, A.K., 2017, Earliest Cretaceous (late Berriasian) glendonites from Northeast Siberia revise the timing of initiation of transient Early Cretaceous cooling in the high latitudes: Cretaceous Research, v. 71, p. 102–112, https://doi.org/10.1016/j.cretres.2016.11.011.

Rogov, M., Ershova, V., Vereshchagin, O., Vasileva, K., Mikhailova, K., and Krylov, A., 2021, Database of global glendonite and ikaite records throughout the Phanerozoic: Earth System Science Data, v. 13, p. 343–356, https://doi.org/10.5194/essd-13-343-2021.

Rosa, E.L.M., and Isbell, J.L., 2021, Late Paleozoic glaciation, *in* Alderton, D., and Elias, S.A., eds., Encyclopedia of Geology (second edition): London, Academic Press, v. 5, p. 534–545, https://doi.org/10.1016/B978-0-08-102908-4.00063-1.

Shekman, Y.D., and Gagen-Torn, G.Y., 1979, State geological map of the USSR, Priokhotie Series, sheet P54-XXXII: Explanatory notes: Moscow, All-Union Scientific Research Institute (VSEGEI), scale 1:200,000, 88 p. (in Russian).

Tremblay, L.B., Schmidt, G.A., Pfirman, S., Newton, R., and DeRepentigny, P., 2015, Is ice-rafted sediment in a North Pole marine record evidence for perennial sea-ice cover?: Philosophical Transactions of the Royal Society, A: Mathematical, Physical, and Engineering Sciences, v. 373, 20140168, https://doi.org/10.1098/rsta.2014.0168

Printed in USA